Eur. Phys. J. A **18**, 401–404 (2003)
DOI 10.1140/epja/i2002-10244-0

**THE EUROPEAN PHYSICAL JOURNAL A**

# Helicity dependence of the $\gamma$N interaction and the GDH sum rule

P. Pedroni[a]

For the GDH and A2 Collaborations
INFN-Sezione di Pavia, via Bassi 6, Pavia, Italy

Received: 30 September 2002 /
Published online: 22 October 2003 – 

**Abstract.** First measurements of pion photoproduction using circularly polarized photons on longitudinally polarized protons were carried out at MAMI (Mainz) in the energy range $E_\gamma = 200$–$800\,\mathrm{MeV}$. Results of the helicity dependence of the total inclusive photoabsorption cross-section and of the pion photoproduction channels will be presented. These data provide new input for multipole analyses and determine the main contribution to the Gerasimov-Drell-Hearn integral and the forward spin polarizability $\gamma_0$.

**PACS.** 13.60.Le Meson production – 14.20.Gk Baryon resonances with $S = 0$

## 1 Introduction

The helicity-dependent total cross-sections for the absorption of real photons on nucleons, $\sigma_{3/2}$ and $\sigma_{1/2}$, corresponding to the two parallel or antiparallel relative spin configurations, respectively, are related to the anomalous magnetic moment $\kappa$ of the nucleon via the Gerasimov-Drell-Hearn (GDH) sum rule [1]:

$$\int_0^\infty \left(\sigma_{3/2} - \sigma_{1/2}\right) \frac{\mathrm{d}\nu}{\nu} = \frac{2\pi\alpha}{m^2}\kappa^2. \qquad (1)$$

In a similar way, the forward spin polarizability $\gamma_0$, a structure constant of the nucleon still unmeasured, can be obtained as

$$\gamma_0 = -\frac{1}{4\pi^2}\int_0^\infty \left(\sigma_{3/2} - \sigma_{1/2}\right) \frac{\mathrm{d}\nu}{\nu^3}\,. \qquad (2)$$

Both equations connect the ground-state properties of the nucleon ($m$, $e$, $\kappa$, $\gamma_0$) with the dynamics of the excitation spectrum.

The GDH sum rule is based on very general physics principles (low-energy theorems, optical theorem, unsubtracted dispersion relation) applied to the Compton forward amplitude and gives important constraints for the models of the nucleon. Due to its fundamental character this prediction, formulated in the 1960s, deserves a verification which has been awaiting technical developments that only recently have taken place.

Apart from the GDH sum rule, another important motivation to study the helicity structure of single- and double-pion photoproduction lies in the fact that it provides completely new and up to now inaccessible information on partial-wave amplitudes. The inclusion of this new observable into multipole analyses will allow to access small resonance amplitudes and help to separate them from the dominating ones and from the non-resonant background.

The aim of the GDH Collaboration[1] is to provide an extensive data set of helicity-dependent cross-sections for all the partial and total reactions channels both on the proton and on the neutron with a combined use of the MAMI (Mainz) ($m_\pi \le E_\gamma \le 800\,\mathrm{MeV}$) and ELSA (Bonn) ($E_\gamma \le 3\,\mathrm{GeV}$) accelerators. In the following, the first results from the Mainz experimental part will be presented.

## 2 Experimental set-up

The experiment was carried out at the tagged-photon facility of the MAMI accelerator in Mainz.

Circularly polarized electrons were produced by bremsstrahlung of longitudinally polarized electrons. The electron source, based on the photoeffect on strained GaAs crystals, delivered routinely electrons with a degree of polarization of $\sim$ 75% [2]. The degree of polarization was continuously measured throughout the experiment by Möller scattering in a magnetized iron foil.

[a] e-mail: pedroni@pv.infn.it

[1] This collaboration is formed by researchers from the Universities of Mainz, Bonn, Bochum, Erlangen, Göttingen, Lund, Nagoya, Pavia, Tübingen and from INFN-Sezione di Pavia, RUG Gent, CEA Saclay, INR Moscow.

Polarized nucleons were available in the frozen-spin target [3] that consisted of a horizontal dilution refrigerator and a superconducting polarization magnet, which was used in the polarization phase together with a microwave system for dynamical nuclear polarization (DNP). The polarization was maintained during the measurement in the "frozen-spin" mode at temperatures of about 50 mK by an internal superconducting coil ($B \simeq 0.4$ T) which is integrated into the dilution refrigerator.

The target material was butanol ($C_4H_9OH$). At 2.5 T maximum polarization values close to 90% were obtained for the protons with a typical relaxation time of about 200 hours.

The photon-induced reaction products were registered by means of the detector DAPHNE [4], made by CEA Saclay and INFN-Sezione di Pavia, which is complemented by forward detectors to increase the solid-angle acceptance. DAPHNE is essentially a charged-particle tracking detector having a cylindrical symmetry. It consists of 3 coaxial layers of multi-wire proportional chambers, surrounded by a segmented $\Delta E$-$E$-$\Delta E$ plastic scintillator telescope and by a double scintillator-absorber sandwich which allows the detection of neutral pions with a useful efficiency.

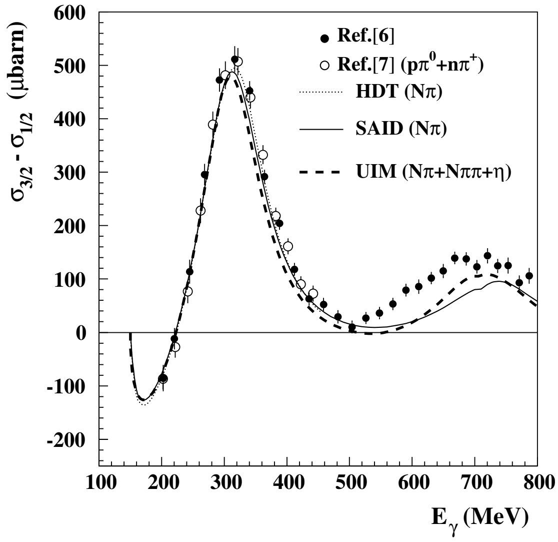


**Fig. 1.** The helicity-dependent total cross-section $\sigma_{3/2} - \sigma_{1/2}$ on $^1$H [6] (filled points) is compared to the sum of the $N\pi$ channels [7] (empty points) and to the predictions of the HDT [8], SAID [9] and UIM [10] analyses. Only statistical errors are shown.

## 3 Results and comments

### 3.1 Inclusive total cross-section

An inclusive method of data analysis has been developed to determine the total absorption cross-section. Its characteristics are fully described in [5,6].

The helicity-dependent total photoabsorption cross-section $\Delta\sigma = (\sigma_{3/2} - \sigma_{1/2})$ on the proton [6] (full circles) is shown in fig. 1. Only statistical errors are shown. The estimated total systematic error is about 6% on the measured $\Delta\sigma$ [6].

These data are compared with the sum of our previously published helicity dependence for the $n\pi^+$ and $p\pi^0$ channels in the $\Delta$ region [7]. The good agreement found between the different analyses gives us confidence in their reliability.

In the same figure the predictions of the HDT [8], SAID [9], and UIM [10] analyses are also shown. In the $\Delta$-resonance region, there is a good agreement between experiment and theories. In the second resonance region, a significant contribution from double-pion photoproduction is clearly visible. This feature is not completely reproduced by the UIM model. The measured value of the GDH integral between 200 and 800 MeV amounts to $226 \pm 5$ (stat) $\pm 12$ (sys) $\mu$b. Due to the $\nu^{-3}$ weighting, the $\gamma_0$ integral is almost saturated by $E_\gamma = 800$ MeV. The value of the $\gamma_0$ integral between 200 and 800 MeV amounts to $(-187 \pm 8 \text{ (stat)} \pm 10 \text{ (sys)}) \cdot 10^{-6}$ fm$^4$.

Although the measured photon energy interval is too narrow to draw any definitive conclusion, a reasonable estimate of the GDH sum rule value can be deduced if we use the existing models for the evaluation of the missing contributions. The UIM model [10] gives a contribution of $-30\,\mu$b for $E_\gamma < 200$ MeV and $+40\,\mu$b for $800 < E_\gamma < 1650$ MeV. For $E_\gamma > 1650$ MeV, ref. [11] gives a contribution of $-26\,\mu$b. The combination of our experimental result with these predictions yields an estimate ($210\,\mu$b) which within the experimental errors is consistent with the GDH sum rule value (1). It should be kept in mind that, especially above $E_\gamma = 800$ MeV, none of the models has yet been validated experimentally and only a measurement in this energy region can lead to a definitive conclusion about the high-energy contribution to the GDH integral. Our collaboration is performing such a measurement at ELSA (Bonn) up to $E_\gamma \simeq 3$ GeV.

In case of the $\gamma_0$ integral (2) the contribution from $E_\gamma < 200$ MeV is important, the UIM prediction being $+104 \cdot 10^{-6}$ fm$^4$. The missing high-energy contribution, according to UIM and ref. [11], is $-3 \cdot 10^{-6}$ fm$^4$ only. The combination with our experimental result gives an estimate of $-86 \cdot 10^{-6}$ fm$^4$ for $\gamma_0$. This value is within the range of values predicted by dispersion theories [12,13].

### 3.2 Exclusive measurements

The identification and the energy determination of the charged particles is performed, with high efficiency ($\geq 80\%$) by the maximum likelihood method described in [14], while neutrons and $\pi^0$'s can only be identified (without any energy determination) with an efficiency of 10–30%. These combined features allow the separation of all the single and double photoproduction channels up to 800 MeV.

As an example, in fig. 2 the helicity-dependent cross-section $(\mathrm{d}\sigma/\mathrm{d}\Omega)_{3/2} - (\mathrm{d}\sigma/\mathrm{d}\Omega)_{1/2}$ for the $\gamma p \rightarrow p\pi^0$ channel as a function of pion scattering angle in the CM system

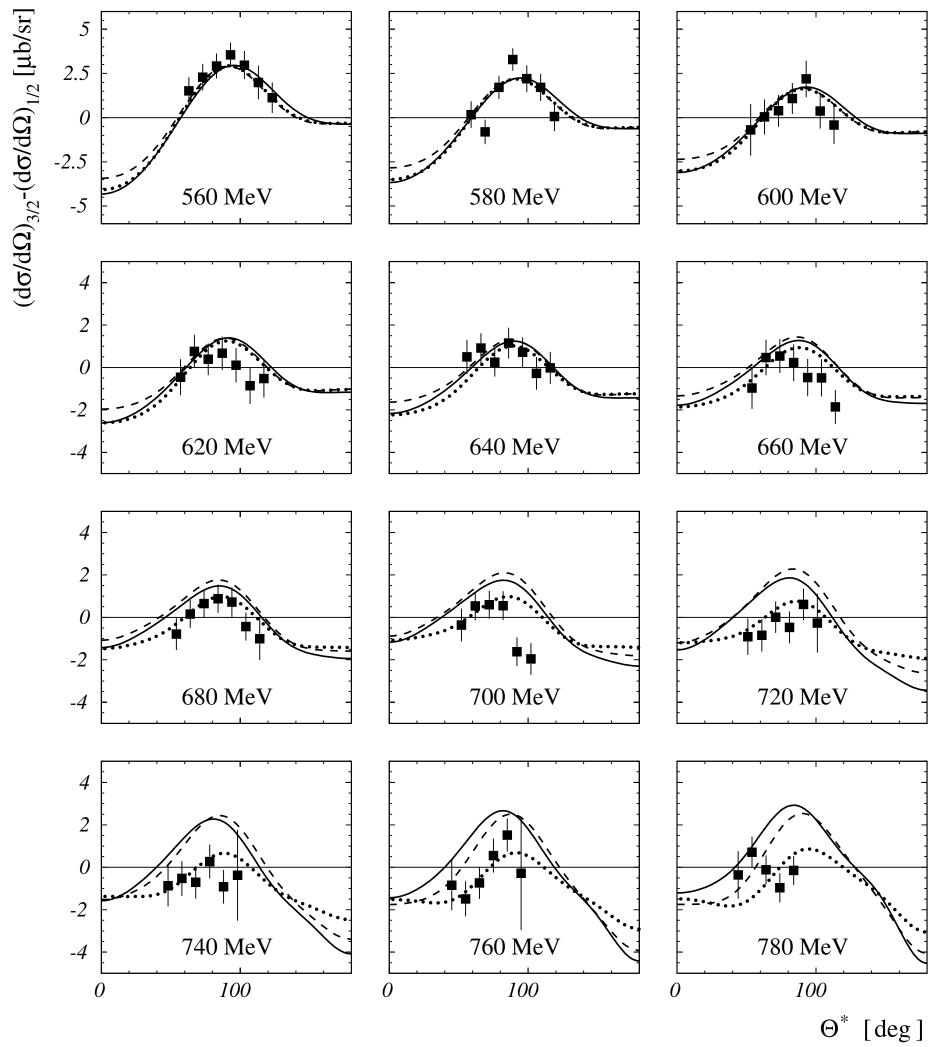


**Fig. 2.** The measured helicity-dependent differential cross-section for $\boldsymbol{\gamma p} \to p\pi^0$ (solid squares) is compared to the SAID [9] (solid line) and UIM [10] (dashed line) analyses. The dotted curve presents the modified solution of UIM (see text). The errors shown are statistical only.

$\theta^*$ is shown in the photon energy region from 550 MeV up to 790 MeV [15].

At the lower photon energies, the data are in a good agreement with SAID and UIM models, while a clear, systematic discrepancy is present when the energy region of the $D_{13}(1520)$-resonance is approached. The dotted line represents a modified UIM solution which was fitted to our data. With respect to the standard UIM solution, the most relevant changes were found for the $M_{2-}^{1/2}$ (11% increase) and $E_{2-}^{1/2}$ (19% decrease) multipoles. This produces a sizeable change in the helicity amplitudes $A_{1/2}$ and $A_{3/2}$, as shown in table 1.

Finally, in fig. 3 [16] the preliminary results for the helicity-dependent total cross-section of all double-pion photoproduction channels on the proton are shown.

According to the existing models [17], the large positive $(\sigma_{3/2}-\sigma_{1/2})$ values for the $p\pi^+\pi^-$ channel, are mainly due to an intermediate excitation of a $\Delta\pi$ state, with the $D_{13}$-resonance playing a minor role. On the contrary, the intermediate excitation of the $D_{13}$ should give the dominant contribution to the $n\pi^+\pi^0$ channel, through the $D_{13} \to n\rho$ decay mode. The intermediate $D_{13}$ excitation is expected to play a major role also for the $p\pi^0\pi^0$ channel (through the $D_{13} \to \Delta\pi$ decay mode) but the small quantity of data analysed up to now for this reaction (about 1/4 of the total statistics) prevents to draw any clear experimental conclusion.

**Table 1.** The $D_{13}$ helicity amplitudes $A_{1/2}$, $A_{3/2}$ for the proton (in units of GeV$^{-1/2}$) estimated from the modified UIM analysis, are compared to the standard UIM solution, and to the PDG latest estimate [18].

| Solution | $A_{1/2}$ | $A_{3/2}$ |
|---|---|---|
| Standard UIM | $-0.017$ | 0.164 |
| PDG estimate | $-0.024 \pm 0.009$ | $0.166 \pm 0.005$ |
| Modified UIM | $-0.038 \pm 0.003$ | $0.147 \pm 0.010$ |

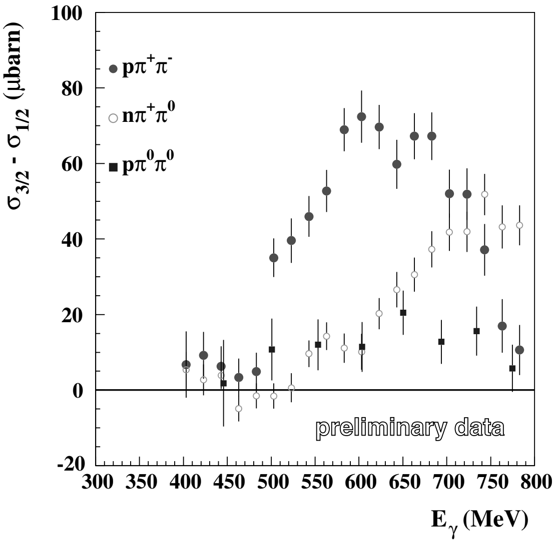


**Fig. 3.** Preliminary helicity-dependent total cross-section ($\sigma_{3/2} - \sigma_{1/2}$) for all $\pi\pi$ photoproduction channels on $^1$H.

## 4 Summary and outlook

First data on the helicity dependence of the photon-nucleon reactions in the energy range from 200 to 800 MeV have been obtained at MAMI.

The helicity dependence of the total cross-section gives valuable information on the nucleon spin structure and allows a test of the GDH sum rule together with a measurement of the forward spin polarizability $\gamma_0$. In addition, new input for multipole analyses is also available from the data on the single- and double-pion production channels.

## References

1. S.B. Gerasimov, Sov. J. Nucl. Phys. **2**, 430 (1966); S.D. Drell, A.C. Hearn, Phys. Rev. Lett. **16**, 430 (1966).
2. K. Aulenbacher *et al.*, Nucl. Instrum. Methods A **391**, 498 (1997).
3. C. Bradtke *et al.*, Nucl. Instrum. Methods A **436**, 430 (1999).
4. G. Audit *et al.*, Nucl. Instrum. Methods. A **301**, 473 (1991).
5. M. Mac Cormick *et al.*, Phys. Rev. C **53**, 41 (1996).
6. J. Ahrens *et al.*, Phys. Rev. Lett. **87**, 02203 (2001).
7. J. Ahrens *et al.*, Phys. Rev. Lett. **84**, 26 (2000).
8. O. Hanstein, Nucl. Phys. A **632**, 561 (1998).
9. R.A. Arndt *et al.*, Phys. Rev. C **53**, 430 (1996), solution SP01.
10. D. Drechsel *et al.*, Nucl. Phys. A **645**, 145 (1999).
11. N. Bianchi, T. Thomas, Phys. Lett. B **450**, 439 (1999).
12. D. Babusci *et al.*, Phys. Rev. C **58**, 1013 (1998).
13. D. Drechsel *et al.*, Phys. Rev. C **61**, 015204 (2000).
14. A. Braghieri *et al.*, Nucl. Instrum. Methods A **343**, 623 (1994).
15. J. Ahrens *et al.*, Phys. Rev. Lett. **88**, 232002 (2002).
16. H. Holvoet, PhD Thesis, University of Gent, 2001; M. Lang, PhD thesis, University of Mainz, in preparation; F. Zapadtka, PhD Thesis, University of Göettingen, in preparation.
17. J.C. Nacher, E. Oset, Nucl. Phys. A **697**, 372 (2002), e-print nucl-th/0106005.
18. D.E. Groom *et al.*, Eur. Phys. J. C **15**, 1 (2000).